Secure Observer-Based H_∞ Synchronization for Singularly Perturbed Multiweighted Complex Networks With Stochastic Communication Protocol

Yan Li, Min Gao, Lijuan Zha, Jinliang Liu, *Senior Member, IEEE*, Engang Tian, *Senior Member, IEEE*, and Chen Peng

***Abstract*—This paper addresses the problem of observer-based H_∞ synchronization control for singularly perturbed multiweighted complex networks (SPMCNs) with communication constraints and cyberattack threats. Firstly, given the limited communication bandwidth, a stochastic communication (SC) protocol is employed to deal with the potential data collision in each node of SPMCNs incurred by the mismatch between traffic load and resource availability. The SC protocol is specifically depicted by a Markov chain with partially known transition probabilities to improve its applicability. Then, the cybersecurity for SPMCNs is investigated, and the focus is concentrated on deception attacks due to they pose significant risks by maliciously tampering with sensitive information. Based on modeling the behavior of the considered deception attacks, observer-assisted synchronization controllers with undetermined gains are designed and an augmented synchronization error system is established. Subsequently, the stability with guaranteed H_∞ control performance of the constructed system is analyzed, and then a feasible algorithm for determining the gains of the desired observers and controllers is provided. Finally, simulations are conducted based on an urban public traffic network to validate the efficiency and practicability of the proposed synchronization control scheme.**

***Index Terms*—Deception attacks, singularly perturbed multiweighted complex networks (SPMCNs), stochastic communication (SC) protocol, synchronization control.**

I. Introduction

RECENTLY, complex networks (CNs) have been acknowledged as a powerful tool for modeling many real-world physical systems with large scale and high complexity such as transportation networks [1], biological networks [2] and industrial networks [3]. In traditional CNs, each link is always assigned with a single weight which represents one kind of relationship between the two connected nodes [4]. However, such single-weighted CNs (SCNs) present apparent limitations in depicting practical systems with different types of interactions between system entities [5]. Towards this end, multiweighted CNs (MCNs), in which each edge is associated with multiple weights, have attracted significant attention from scholars [6], [7]. In engineering applications, MCNs are widely used in fields such as power grids, social networks and biological systems, where numerous types of relationships between nodes coexist and influence the overall system behavior. Moreover, it is noteworthy that the states of many CNs now present two-time-scale feature, i.e., the system behavior is governed by both slow and fast dynamics, which will result in particular difficulties in system control and analysis [8]. To address this issue, singularly perturbed CNs are raised with employing singularly perturbed parameter (SPP) to distinguish the system states on different time scales [9]. In the literature, lots of results focusing on singularly perturbed SCNs (SPSCNs) have been presented [10], [11], but the studies on singularly perturbed MCNs (SPMCNs) are rarely reported, which is the essential motivation of our work.

While initiating the specific exploration on SPMCNs, synchronization which refers to coordinate the dynamics of individual nodes is a critical issue, as it can ensure system stability and efficiency [12], [13]. Actually, various types of synchronization methods, e.g., pinning synchronization [14], lag synchronization [15] and H_∞ synchronization [16], have been proposed for MCNs. Given that the external disturbances and system uncertainties are generally unavoidable in practice, H_∞ synchronization obtains significant concerns since that it dedicates to minimize the worst-case impacts of the mentioned factors on the synchronization process. As an illustration, the authors in [17] designed an H_∞ output synchronization control scheme for MCNs based on Barbalat Lemma; the finite time H_∞ synchronization problem of MCNs with disturbances and adaptive coupling delays was discussed in [18]; for multi derivative coupled MCNs, the Lag H_∞ synchronization issue was studied in [19]. Nevertheless, all the works are conducted in single time scale. Thus, by orienting on two-time-scale scenario

Received 18 February 2025; revised 21 June 2025; accepted 8 July 2025. Date of publication 10 July 2025; date of current version 23 July 2025. This work was supported in part by the National Natural Science Foundation of China under Grant 62373252 and Grant 62273174 and in part by the Natural Science Foundation of Jiangsu Province of China under Grant BK20230063. The associate editor coordinating the review of this article and approving it for publication was Dr. Elif Vural. *(Corresponding author: Jinliang Liu.)*

Yan Li and Min Gao are with the College of Computer Science and Artificial Intelligence, Nanjing University of Finance and Economics, Nanjing 210023, China (e-mail: ylnjue@163.com; gaomin0429@163.com).

Lijuan Zha is with the College of Science, Nanjing Forestry University, Nanjing 210037, China (e-mail: zhalijuan@vip.163.com).

Jinliang Liu is with the School of Computer Science, Nanjing University of Information Science and Technology, Nanjing 210044, China (e-mail: liujinliang@vip.163.com).

Engang Tian is with the School of Optical-Electrical and Computer Engineering, University of Shanghai for Science and Technology, Shanghai 200093, China (e-mail: tianengang@163.com).

Chen Peng is with the School of Mechatronic Engineering and Automation, Shanghai University, Shanghai 200444, China (e-mail: c.peng@shu.edu.cn).

Digital Object Identifier 10.1109/TSIPN.2025.3588094

2373-776X © 2025 IEEE. All rights reserved, including rights for text and data mining, and training of artificial intelligence and similar technologies. Personal use is permitted, but republication/redistribution requires IEEE permission. See https://www.ieee.org/publications/rights/index.html for more information.

Authorized licensed use limited to: Southeast University. Downloaded on July 23,2025 at 23:21:32 UTC from IEEE Xplore. Restrictions apply.

and considering the fact that it is hard to measure system states precisely, we will investigate observer-based H_∞ synchronization for SPMCNs in this paper, which is untouched in the existed researches to the best of our knowledge.

To design synchronization method for SPMCNs, the information exchange among system components should be concerned undoubtedly. It can be observed that the communication is now mainly carried out via wired or wireless networks to achieve efficiency, robustness, and scalability [20]. But due to the continuous increase in network traffic, the bandwidth limitation issue is becoming severe [21]. Then, data collision is likely incurred while multiple sensors deployed in one node of SPMCNs try to send their generated data simultaneously. For addressing the challenge, many communication protocols, typically including round robin (RR) protocol [22], weighted try-once-discard (WTOD) protocol [23], and stochastic communication (SC) protocol [24], are proposed to assure that only one competitor can access the network at each time instant. Among them, SC protocol exhibits improved flexibility and adaptability by leveraging probabilistic decision-making scheme [25]. Moreover, to achieve systematic and predictable data scheduling, Markov chains are extensively used to model the random sequence of access in SC protocol [26]. The conventional works on Markov chains-based SC protocol assume that the transition probabilities of Markov chains are completely known in advance [24], which is often impractical in dynamic environments. Thus, Markov chains with partially known transition probabilities have been exploited to depict SC protocol, and thereby the enhanced flexibility and applicability of SC protocol can be achieved. However, the synchronization issue of SPMCNs with Markov chains-based SC protocol has not been addressed, not to mention to consider the incompleteness of the transition probabilities, which also activates our study.

In addition to the challenge posed by limited communication resources, cyberattacks also make significant difficulties in synchronization control of networked SPMCNs. Given the impact of cyberattacks on system performance, numerous studies have been conducted to explore effective mitigation strategies based on analyzing the nature of different attacks [27], [28]. In practice, deception attacks [29], denial-of-service (DoS) attacks [30], and false data injection (FDI) attacks [31] are recognized as three typical types of cyber threats. From the perspectives of concealment and long-term effects, deception attacks require extra attention as they always try to alter original data with malicious content and thus can hardly be detected. Concentrating on CNs subject to deception attacks, secure synchronization control methods have been explored in the literature. For example, an impulsive controller was designed in [32] to assure secure cluster synchronization of CNs under deception attacks; mean-square bounded synchronization problem over CNs with deception attacks and discontinuous nodes was investigated in [33]; taking coupling delay, data collision and deception attacks into account, secure RR-based synchronization control approach was proposed for CNs in [34]. Differing from the aforementioned studies that focus on SCNs, some researches on synchronization issue of MCNs under deception attacks have also been presented [35], [36], but none of them considers the influences of two-time-scale dynamics and data conflict induced by limited communication resources.

In light of the above discussion, this paper dedicates to devise an observer-based synchronization control method for SPMCNs affecting by potential data collision and deception attacks. The main contributions of the work can be outlined as below.

- Distributed observer-based H_∞ synchronization problem for SPMCNs is studied for the first time, moreover, the impacts of two kinds of network-induced phenomena, i.e., data collision and cyberattacks, are considered integratedly while achieving the desired synchronization.
- The measurement output of each node in the considered SPMCN is effectively described based on appropriately depicting the function of the SC protocol used for data scheduling and the behavior of deception attacks occurring on sensor-observer channels, and the framework of the envisioned distributed observer-based synchronization controllers is proposed accordingly.
- A novel augmented system model is constructed by grouping the formulated dynamics of all nodes in the SPMCN, following which the distributed observers and controllers' gains are derived via analyzing the ϵ-independent conditions for the stability and guaranteed H_∞ control performance of the established system.
- A practical urban public traffic network is modeled by the described SPMCN, and extensive simulations are thereby conducted to verify the effectiveness and applicability of the designed synchronization control strategy.

The rest of the paper is organized as follows. In Section II, the system model and complicated network environment are firstly depicted, then the formulation of the studied synchronization problem over the envisioned SPMCN is presented. In Section III, the sufficient conditions ensuring the desired synchronization control performance of the SPMCN are investigated, and then the feasible solution to the gains of the synchronization controllers is obtained. In Section IV, simulation results are displayed and analyzed to verify the effectiveness of our study in addressing the synchronization control issue. The conclusion of the paper is given in Section V.

II. System Model and Problem Description

In this section, the basic model of the considered SPMCN is introduced firstly. Then, the adopted SC protocol using for mitigating data conflict and the considered deception attacks affecting data security are specifically described, which is followed by the formulation of the designed observer-based synchronization controllers. Finally, the studied problem is explicitly depicted based on constructing an augmented synchronization error system.

A. Model of the SPMCN

We consider a discrete time SPMCN with N homogeneous nodes, i.e., $node_1$, $node_2$,..., $node_N$. Thus, without loss of generality, the following introduction will focus on $node_i$. For the node, the specific architecture is shown in Fig. 1, and the

Authorized licensed use limited to: Southeast University. Downloaded on July 23,2025 at 23:21:32 UTC from IEEE Xplore. Restrictions apply.

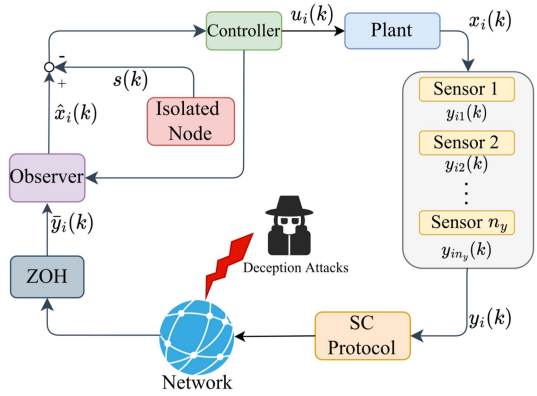

Fig. 1. The structure of $node_i$ in the considered SPMCN.

model is given as below.

$$\begin{cases} x_i(k+1) = AE_\epsilon x_i(k) + c_1 \sum_{j=1}^{N} \theta_{ij}^1 \Gamma_1 E_\epsilon x_j(k) + c_2 \\ \qquad \times \sum_{j=1}^{N} \theta_{ij}^2 \Gamma_2 E_\epsilon x_j(k) + \cdots + c_l \sum_{j=1}^{N} \theta_{ij}^l \Gamma_l \\ \qquad \times E_\epsilon x_j(k) + Bu_i(k) + Hw_i(k) \\ y_i(k) = Cx_i(k) + Dw_i(k) \end{cases} \tag{1}$$

where $x_i(k) \in \mathbb{R}^{n_x}$ is the system state vector which is composed by the slow vector $x_{is}(k) \in \mathbb{R}^{n_s}$ and fast vector $x_{if}(k) \in \mathbb{R}^{n_f}$ $(n_s + n_f = n_x)$; $y_i(k) \in \mathbb{R}^{n_y}$ and $u_i(k) \in \mathbb{R}^{n_u}$ represent the measurement output and control input, respectively; $w_i(k) \in \mathbb{R}^{n_\omega}$ denotes the external disturbance that lies in $\mathbb{L}_2[0,\infty)$; $E_\epsilon \triangleq \text{diag}\{I_{n_s}, \epsilon I_{n_f}\}$ is the singularly perturbed matrix with the SPP $\epsilon \in (0, \bar{\epsilon}]$, and $\bar{\epsilon}$ is the upper bound of the SPP; A, B, C, D and H are known matrices with real numbers and appropriate dimensions; l represents the number of weights of the SPMCN, then for each weight, e.g., the m-th weight $(1 \le m \le l)$, c_m is the coupling strength; $\Gamma_m = diag\{\mu_m^1, \mu_m^2, \ldots, \mu_m^{n_x}\}$ indicates the constant inner-coupling matrix, where $\mu_m^d \neq 0$ $(1 \le d \le n_x)$ denotes that two coupled nodes are connected via the d-th component of the corresponding state variable; $\Theta_m = [\theta_{ij}^m]_{N\times N}$ is the outer-coupling matrix employed for representing the coupling framework of the SPMCN, in which $\theta_{ij}^m \ge 0$ $(1 \le i \ne j \le N)$ describes the relationship between $node_i$ and $node_j$, i.e., $\theta_{ij}^m > 0$ if there is a connection between the two nodes, otherwise $\theta_{ij}^m = 0$, and θ_{ii}^m is set to be $-\sum_{j=1,j\neq i}^{N} \theta_{ij}^m$; apparently, the interactions between nodes in the SPMCN are comprehensively depicted by the inner-coupling and outer-coupling matrices.

B. The SC Protocol Driven by Markov Chain

As shown in Fig. 1, the measurement output $y_i(k)$ is assumed to be discerned by n_y sensors for comprehensiveness, i.e., $y_i(k) = [y_{i1}(k), y_{i2}(k), \ldots, y_{in_y}(k)]^T$. To avoid data collision incurred by the limited network bandwidth, SC protocol is then employed to arrange the data transmission of n_y sensors and thus assuring that only one dimension of $y_i(k)$ can be released into the shared network at each time instant. By further applying the zero-order-holder (ZOH) technique, the signal updating standard for the s-th sensor $(s \in \mathbb{M}^i = \{1, 2, \ldots, n_y\})$ can be described as

$$\bar{y}_{is}(k) = \begin{cases} y_{is}(k), & s = \psi_i(k) \\ \bar{y}_{is}(k-1), & \text{otherwise} \end{cases} \tag{2}$$

where $\psi_i(k) \in \mathbb{M}^i$ represents the index of the sensor that is allowed to transmit its generated data based on the adopted SC protocol which will be introduced shortly.

Remark 1: Although the introducing of the SC protocol may lead to unreliable measurement output as only one sensor can transmit its signal at each time instant, it effectively mitigates data collision which would otherwise result in complete data loss due to the limited communication bandwidth. Additionally, the ZOH strategy, which works by using the most recent stored data to compensate for signals from sensors that are not permitted to access the network, is employed under the SC protocol as reflected in (2). Comparing with the zero-input (ZI) strategy which updates the signals of unscheduled sensors to be zero [37], the ZOH strategy ensures the continuity of signal transmission and thereby enhances the stability and reliability of the system [24], [38].

For the SC protocol, a Markov chain with a transition probability matrix $P^i = [\pi_{qh}^i] \in \mathbb{R}^{n_y \times n_y}$ is used to adjust the variable $\psi_i(k)$, where $\pi_{qh}^i \in [0,1]$ and $\sum_{h=1}^{n_y} \pi_{qh}^i = 1$ for $\forall q \in \mathbb{M}^i$. Then, the transition probability of $\psi_i(k)$ is established as

$$\text{Prob}\{\psi_i(k+1) = h | \psi_i(k) = q\} = \pi_{qh}^i. \tag{3}$$

In other words, the probability that selecting sensor h at time instant $k+1$ while sensor q is scheduled at time instant k is set to be π_{qh}^i. In addition, we assume that the transition probabilities of the Markov chain are partially known, e.g., P^i can be represented as

$$P^i = \begin{bmatrix} \pi_{11}^i & \pi_{12}^i & \cdots & ? \\ ? & ? & \cdots & \pi_{2n_y}^i \\ \vdots & \vdots & \ddots & \vdots \\ \pi_{n_y 1}^i & ? & \cdots & \pi_{n_y n_y}^i \end{bmatrix} \tag{4}$$

where "?" indicates an unknown transition probability. Under such circumstance, for $\forall q \in \mathbb{M}^i$, the set $\mathbb{M}^i$ can be divided as

$$\mathbb{M}^i = \mathbb{M}_{\mathcal{K}q}^i \cup \mathbb{M}_{\mathcal{U}.\mathcal{K}.q}^i \tag{5}$$

with

$$\mathbb{M}_{\mathcal{K}q}^i \triangleq \{h : \pi_{qh}^i \text{is known}\}, \quad \mathbb{M}_{\mathcal{U}.\mathcal{K}.q}^i \triangleq \{h : \pi_{qh}^i \text{is unknown}\}.$$

Remark 2: Actually, SC protocol has been widely used for many applications such as traffic routing in wireless networks, user scheduling in cognitive radio networks and signal transmission in vehicular systems. In this study, the SC protocol driven by the described Markov chain is adopted for each $node_i$ to schedule the measurement output generated by n_y sensors. Moreover, it is essential to recognize that in (5), if $\mathbb{M}_{\mathcal{U}.\mathcal{K}.q}^i = \emptyset$ for all q, then the Markov chain is reduced into the traditional case that the transition probabilities are completely known [38], [39]; if $\mathbb{M}_{\mathcal{K}q}^i = \emptyset$ for all q, then it corresponds to a situation that the transition probabilities for the Markov chain are completely unknown which has been explored in [40]. However, considering

Authorized licensed use limited to: Southeast University. Downloaded on July 23,2025 at 23:21:32 UTC from IEEE Xplore. Restrictions apply.

that some transition probabilities can still be inferred via observation and data analysis although it is hard to obtain complete information in practice, our adopted Markov chain with partially known transition probabilities is more general and realistic.

C. Formulation of the Considered Deception Attacks

While delivering the released measurement output over the communication network, it is noteworthy that the network bandwidth is now generally divided into multiple channels for realizing fine-grained bandwidth sharing, and then the network may be compromised by asynchronous cyberattacks [41], [42]. In view of this, we will consider the scenario that each $node_i$ in the envisioned SPMCN is subjected to a different deception attack which is denoted by DA_i in this study. For DA_i, a Bernoulli variable $\alpha_i(k)$ with the following probability is firstly used to describe the occurrence of it.

$$\text{Prob}\{\alpha_i(k)=1\}=\bar{\alpha}_i,\quad \text{Prob}\{\alpha_i(k)=0\}=1-\bar{\alpha}_i. \tag{6}$$

Specifically, $\alpha_i(k)=1$ indicates that DA_i is launched at time instant k and then the released signal will be affected; otherwise the transmitted signal $y_{i\psi_i(k)}(k)$ can be successfully received by the observer. Moreover, the attack signal $\phi_i(k)=[\phi_{i1}(k),\phi_{i2}(k),\ldots,\phi_{in_y}(k)]^T$ with the following condition is assumed to be generated by the attacker.

$$\|\phi_i(k)\|\le\|Wx_i(k)\| \tag{7}$$

where W is a given matrix with a suitable dimension.

Taking the above formulated attack into account, the measurement signal presented in (2) can be renewed as

$$\bar{y}_{is}(k)=\begin{cases}y_{is}(k)+\alpha_i(k)(-y_{is}(k)+\phi_{is}(k)), & s=\psi_i(k)\\ \bar{y}_{is}(k-1), & \text{otherwise.}\end{cases} \tag{8}$$

For the convenience of subsequent analysis, we further denote $\bar{y}_i(k)=[\bar{y}_{i1}(k),\bar{y}_{i2}(k),\ldots,\bar{y}_{in_y}(k)]^T$ and introduce the Kronecker delta function $\delta(\cdot)\in\{0,1\}$ to get that

$$\begin{aligned}\bar{y}_i(k)=&(1-\alpha_i(k))\Phi_{\psi_i(k)}y_i(k)+(I_{n_y}-\Phi_{\psi_i(k)})\bar{y}_i(k-1)\\&+\alpha_i(k)\Phi_{\psi_i(k)}\phi_i(k)\end{aligned} \tag{9}$$

where $\Phi_{\psi_i(k)}=diag\{\delta(\psi_i(k)-1),\ldots,\delta(\psi_i(k)-n_y)\}$, I_{n_y} represents the identity matrix with dimension n_y.

Remark 3: In practice, deception attacks are not always successfully launched due to the construction of defense mechanisms and limitation of network conditions, and then present stochastic feature. Thus, it is reasonable to use the Bernoulli process to depict each DA_i, and the probability $\bar{\alpha}_i$ can be determined based on long-term monitoring and assessment [43]. Furthermore, $\phi_i(k)$ satisfied the condition (7) is employed to formulate the specific influence of DA_i given that the energy-bounded attack signals can enhance the stealthiness of the attack behavior [34].

D. Model of the Observer and Synchronization Controller

Given that it is difficult to obtain accurate state of each $node_i$ in the SPMCN, the following observer is firstly presented.

$$\begin{cases}\hat{x}_i(k+1)=AE_\epsilon\hat{x}_i(k)+c_1\sum_{j=1}^N\theta_{ij}^1\Gamma_1E_\epsilon\hat{x}_j(k)+c_2\\ \qquad\times\sum_{j=1}^N\theta_{ij}^2\Gamma_2E_\epsilon\hat{x}_j(k)+\cdots+c_l\sum_{j=1}^N\theta_{ij}^l\Gamma_l\\ \qquad\times E_\epsilon\hat{x}_j(k)+Bu_i(k)+L_{i,\psi_i(k)}(\bar{y}_i(k)-\hat{y}_i(k))\\ \hat{y}_i(k)=C\hat{x}_i(k)\end{cases} \tag{10}$$

where $\hat{x}_i(k)\in\mathbb{R}^{n_x}$ and $\hat{y}_i(k)\in\mathbb{R}^{n_y}$ are the estimated system state and measurement output, respectively, $L_{i,\psi_i(k)}$ represents the observer gain which needs to be determined.

As shown in Fig. 1, an isolated node with the following dynamics is co-located with $node_i$.

$$s(k+1)=AE_\epsilon s(k) \tag{11}$$

then the synchronization of the SPMCN can be achieved by synchronizing each $node_i$ with the isolated node. Based on (10) and (11), the synchronization controller is designed as

$$u_i(k)=K_{i,\psi_i(k)}(\hat{x}_i(k)-s(k)) \tag{12}$$

where $K_{i,\psi_i(k)}$ is the controller gain which will be decided shortly.

E. Problem Formulation

We define the observer error and synchronization error as $e_i(k)=x_i(k)-\hat{x}_i(k)$ and $\bar{e}_i(k)=x_i(k)-s(k)$, respectively, then it can be obtained that

$$\begin{aligned}&e_i(k+1)=x_i(k+1)-\hat{x}_i(k+1)\\&=AE_\epsilon x_i(k)+c_1\sum_{j=1}^N\theta_{ij}^1\Gamma_1E_\epsilon x_j(k)+c_2\sum_{j=1}^N\theta_{ij}^2\Gamma_2E_\epsilon x_j(k)\\&\quad+\cdots+c_l\sum_{j=1}^N\theta_{ij}^l\Gamma_lE_\epsilon x_j(k)+Bu_i(k)+Hw_i(k)-AE_\epsilon\\&\quad\times\hat{x}_i(k)-c_1\sum_{j=1}^N\theta_{ij}^1\Gamma_1E_\epsilon\hat{x}_j(k)-c_2\sum_{j=1}^N\theta_{ij}^2\Gamma_2E_\epsilon\hat{x}_j(k)\\&\quad+\cdots-c_l\sum_{j=1}^N\theta_{ij}^l\Gamma_lE_\epsilon\hat{x}_j(k)-Bu_i(k)-L_{i,\psi_i(k)}(\bar{y}_i(k)\\&\quad-\hat{y}_i(k))\\&=AE_\epsilon e_i(k)+c_1\sum_{j=1}^N\theta_{ij}^1\Gamma_1E_\epsilon e_j(k)+c_2\sum_{j=1}^N\theta_{ij}^2\Gamma_2E_\epsilon e_j(k)\\&\quad+\cdots+c_l\sum_{j=1}^N\theta_{ij}^l\Gamma_lE_\epsilon e_j(k)+Hw_i(k)-L_{i,\psi_i(k)}(\bar{y}_i(k)\\&\quad-\hat{y}_i(k))\\&=AE_\epsilon e_i(k)+c_1\sum_{j=1}^N\theta_{ij}^1\Gamma_1E_\epsilon e_j(k)+c_2\sum_{j=1}^N\theta_{ij}^2\Gamma_2E_\epsilon e_j(k)\end{aligned}$$

Authorized licensed use limited to: Southeast University. Downloaded on July 23,2025 at 23:21:32 UTC from IEEE Xplore. Restrictions apply.

$$+\cdots+c_l\sum_{j=1}^{N}\theta_{ij}^{l}\Gamma_l E_\epsilon e_j(k)+Hw_i(k)-L_{i,\psi_i(k)}[(1-\alpha_i(k))\Phi_{\psi_i(k)}(Cx_i(k)+Dw_i(k))+(I-\Phi_{\psi_i(k)})\bar{y}_i(k-1)+\alpha_i(k)\Phi_{\psi_i(k)}\phi_i(k)]+L_{i,\psi_i(k)}C(x_i(k)-e_i(k)) \quad (13)$$

$$\bar{e}_i(k+1)=x_i(k+1)-s(k+1)$$

$$=AE_\epsilon x_i(k)+c_1\sum_{j=1}^{N}\theta_{ij}^{1}\Gamma_1E_\epsilon x_j(k)+c_2\sum_{j=1}^{N}\theta_{ij}^{2}\Gamma_2E_\epsilon x_j(k)+\cdots+c_l\sum_{j=1}^{N}\theta_{ij}^{l}\Gamma_lE_\epsilon x_j(k)+BK_{i,\psi_i(k)}(\hat{x}_i(k)-s(k))+H\times w_i(k)-AE_\epsilon s(k)$$

$$=AE_\epsilon\bar{e}_i(k)+c_1\sum_{j=1}^{N}\theta_{ij}^{1}\Gamma_1E_\epsilon\bar{e}_j(k)+c_2\sum_{j=1}^{N}\theta_{ij}^{2}\Gamma_2E_\epsilon\bar{e}_j(k)+\ldots+c_l\sum_{j=1}^{N}\theta_{ij}^{l}\Gamma_lE_\epsilon\bar{e}_j(k)+BK_{i,\psi_i(k)}\bar{e}_i(k)-BK_{i,\psi_i(k)}\times e_i(k)+Hw_i(k). \quad (14)$$

For the subsequent analysis, we integrate the information of N nodes and then get that

$$x(k+1)=\widetilde{A}\widetilde{E}_\epsilon x(k)+c_1\widetilde{G}_1\widetilde{E}_\epsilon x(k)+c_2\widetilde{G}_2\widetilde{E}_\epsilon x(k)+\cdots+c_l\widetilde{G}_l\widetilde{E}_\epsilon x(k)+\widetilde{B}u(k)+\widetilde{H}w(k)$$
$$=(\widetilde{A}+c_1\widetilde{G}_1+c_1\widetilde{G}_1+\ldots+c_l\widetilde{G}_l)\widetilde{E}_\epsilon x(k)+\widetilde{B}\times u(k)+\widetilde{H}w(k) \quad (15)$$

$$\bar{y}(k)=(\widetilde{I}-\alpha(k))\widetilde{\Phi}_{\psi(k)}y(k)+(\widetilde{I}-\widetilde{\Phi}_{\psi(k)})\bar{y}(k-1)+\alpha(k)\times\widetilde{\Phi}_{\psi(k)}\phi(k)$$
$$=(\widetilde{I}-\alpha(k))\widetilde{\Phi}_{\psi(k)}\widetilde{C}x(k)+(\widetilde{I}-\alpha(k))\widetilde{\Phi}_{\psi(k)}\widetilde{D}w(k)+(\widetilde{I}-\widetilde{\Phi}_{\psi(k)})\bar{y}(k-1)+\alpha(k)\widetilde{\Phi}_{\psi(k)}\phi(k) \quad (16)$$

$$e(k+1)=\widetilde{A}\widetilde{E}_\epsilon e(k)+c_1\widetilde{G}_1\widetilde{E}_\epsilon e(k)+c_2\widetilde{G}_2\widetilde{E}_\epsilon e(k)+\ldots+c_l\widetilde{G}_l\widetilde{E}_\epsilon e(k)+\widetilde{H}w(k)-\widetilde{L}_{\psi(k)}[(\widetilde{I}-\alpha(k))\widetilde{\Phi}_{\psi(k)}\times(\widetilde{C}x(k)+\widetilde{D}w(k))+(\widetilde{I}-\widetilde{\Phi}_{\psi(k)})\bar{y}(k-1)+\alpha(k)\times\widetilde{\Phi}_{\psi(k)}\phi(k)]+\widetilde{L}_{\psi(k)}\widetilde{C}(x(k)-e(k))$$
$$=[(\widetilde{A}+c_1\widetilde{G}_1+c_2\widetilde{G}_2+\ldots+c_l\widetilde{G}_l)\widetilde{E}_\epsilon-\widetilde{L}_{\psi(k)}\widetilde{C}]\times e(k)+(\widetilde{L}_{\psi(k)}\widetilde{C}-(\widetilde{I}-\alpha(k))\widetilde{L}_{\psi(k)}\widetilde{\Phi}_{\psi(k)}\widetilde{C})x(k)+(\widetilde{H}-(\widetilde{I}-\alpha(k))\widetilde{L}_{\psi(k)}\widetilde{\Phi}_{\psi(k)}\widetilde{D})w(k)-\widetilde{L}_{\psi(k)}(\widetilde{I}-\widetilde{\Phi}_{\psi(k)})\bar{y}(k-1)-\alpha(k)\widetilde{L}_{\psi(k)}\widetilde{\Phi}_{\psi(k)}\phi(k) \quad (17)$$

$$\bar{e}(k+1)=[(\widetilde{A}+c_1\widetilde{G}_1+c_2\widetilde{G}_2+\ldots+c_l\widetilde{G}_l)\widetilde{E}_\epsilon+\widetilde{B}\times\widetilde{K}_{\psi(k)}]\bar{e}(k)-\widetilde{B}\widetilde{K}_{\psi(k)}e(k)+\widetilde{H}w(k) \quad (18)$$

where

$$x(k)=col_N\{x_i(k)\},\quad \bar{y}(k)=col_N\{\bar{y}_i(k)\}$$
$$e(k)=col_N\{e_i(k)\},\quad \bar{e}(k)=col_N\{\bar{e}_i(k)\}$$
$$w(k)=col_N\{w_i(k)\},\quad \phi(k)=col_N\{\phi_i(k)\}$$
$$u(k)=col_N\{u_i(k)\},\quad \widetilde{A}=diag\{A,A,\ldots,A\}$$
$$\widetilde{B}=diag\{B,B,\ldots,B\},\quad \widetilde{C}=diag\{C,C,\ldots,C\}$$
$$\widetilde{D}=diag\{D,D,\ldots,D\},\quad \widetilde{H}=diag\{H,H,\ldots,H\}$$
$$\widetilde{E}_\epsilon=diag\{E_\epsilon,E_\epsilon,\ldots,E_\epsilon\},\quad \widetilde{I}=diag\{I_{n_y},\ldots,I_{n_y}\}$$
$$\widetilde{G}_m=[\theta_{ij}^{m}]_{N\times N}\otimes\Gamma_m$$
$$\alpha(k)=diag\{\alpha_1(k),\alpha_2(k),\ldots,\alpha_N(k)\}$$
$$\widetilde{\Phi}_{\psi(k)}=diag\{\Phi_{1,\psi_1(k)},\Phi_{2,\psi_2(k)},\ldots,\Phi_{N,\psi_N(k)}\}$$
$$\widetilde{L}_{\psi(k)}=diag\{L_{1,\psi_1(k)},L_{2,\psi_2(k)},\ldots,L_{N,\psi_N(k)}\}$$
$$\widetilde{K}_{\psi(k)}=diag\{K_{1,\psi_1(k)},K_{2,\psi_2(k)},\ldots,K_{N,\psi_N(k)}\}$$
$$\psi(k)=1,2,\ldots,z,\quad z={n_y}^{N}.$$

By summarizing up (15)–(18), an augmented synchronization error system can be constructed as below.

$$\chi(k+1)=(\mathcal{M}_1+\mathcal{M}_2)\chi(k)+(\mathcal{N}_1+\mathcal{N}_2)\mathcal{U}(k) \quad (19)$$

where

$$\chi(k)=\begin{bmatrix}x^T(k) & e^T(k) & \bar{e}^T(k) & \bar{y}^T(k-1)\end{bmatrix}^T$$
$$\mathcal{U}(k)=\begin{bmatrix}w^T(k) & \phi^T(k)\end{bmatrix}^T$$
$$\mathcal{M}_1=\begin{bmatrix}\Upsilon_1 & -\widetilde{B}\widetilde{K}_{\psi(k)} & \widetilde{B}\widetilde{K}_{\psi(k)} & 0\\ \Upsilon_2 & \Upsilon_3 & 0 & \Upsilon_4\\ 0 & -\widetilde{B}\widetilde{K}_{\psi(k)} & \Upsilon_1+\widetilde{B}\widetilde{K}_{\psi(k)} & 0\\ \Upsilon_5 & 0 & 0 & \widetilde{I}-\widetilde{\Phi}_{\psi(k)}\end{bmatrix}$$
$$\mathcal{M}_2=\begin{bmatrix}\mathcal{R}_1 & 0 & 0 & 0\end{bmatrix}$$
$$\mathcal{N}_1=\begin{bmatrix}\widetilde{H} & 0\\ \widetilde{H}-\vec{\alpha}\widetilde{L}_{\psi(k)}\widetilde{\Phi}_{\psi(k)}\widetilde{D} & -\vec{\alpha}\widetilde{L}_{\psi(k)}\widetilde{\Phi}_{\psi(k)}\\ \widetilde{H} & 0\\ \vec{\alpha}\widetilde{\Phi}_{\psi(k)}\widetilde{D} & \bar{\alpha}\widetilde{\Phi}_{\psi(k)}\end{bmatrix}$$
$$\mathcal{N}_2=\begin{bmatrix}0 & 0\\ \tilde{\alpha}(k)\widetilde{L}_{\psi(k)}\widetilde{\Phi}_{\psi(k)}\widetilde{D} & -\tilde{\alpha}(k)\widetilde{L}_{\psi(k)}\widetilde{\Phi}_{\psi(k)}\\ 0 & 0\\ \tilde{\alpha}(k)\widetilde{\Phi}_{\psi(k)}\widetilde{D} & \tilde{\alpha}(k)\widetilde{\Phi}_{\psi(k)}\end{bmatrix}$$
$$\Upsilon_1=(\widetilde{A}+c_1\widetilde{G}_1+c_2\widetilde{G}_2+\cdots+c_l\widetilde{G}_l)\widetilde{E}_\epsilon$$
$$\Upsilon_2=\widetilde{L}_{\psi(k)}\widetilde{C}-\vec{\alpha}\widetilde{L}_{\psi(k)}\widetilde{\Phi}_{\psi(k)}\widetilde{C},\quad \Upsilon_3=\Upsilon_1-\widetilde{L}_{\psi(k)}\widetilde{C}$$
$$\Upsilon_4=-\widetilde{L}_{\psi(k)}(\widetilde{I}-\widetilde{\Phi}_{\psi(k)}),\quad \Upsilon_5=\vec{\alpha}\widetilde{\Phi}_{\psi(k)}\widetilde{C}$$

Authorized licensed use limited to: Southeast University. Downloaded on July 23,2025 at 23:21:32 UTC from IEEE Xplore. Restrictions apply.

$$\mathcal{R}_1 = \begin{bmatrix} 0 & \tilde{\alpha}(k)\widetilde{C}^T\widetilde{\Phi}^T_{\psi(k)}\widetilde{L}^T_{\psi(k)} & 0 & -\tilde{\alpha}(k)\widetilde{C}^T\widetilde{\Phi}^T_{\psi(k)} \end{bmatrix}^T$$

$$\bar{\alpha} = diag\{\bar{\alpha}_1, \bar{\alpha}_2, \ldots, \bar{\alpha}_N\}$$

$$\vec{\alpha} = \widetilde{I} - \bar{\alpha}, \quad \tilde{\alpha}(k) = \alpha(k) - \bar{\alpha}.$$

On the basis of the established system, the synchronization of the considered SPMCN can be achieved with the guarantee of the stability of the system (19), which will be specifically discussed shortly. At the end of the section, the following definitions and lemmas are presented to assist the subsequent derivation.

Definition 1: [44] For the system (19) with an initial value $\chi(0)$, under $w(k) \equiv 0$, if there exists a matrix $\mathcal{I} > 0$ which can assure that

$$E\left\{\sum_{k=0}^{\infty} ||\chi(k)||^2|_{\chi(0)}\right\} \leq \chi^T(0)\mathcal{I}\chi(0)$$

then the system is stochastically stable.

Definition 2: [45] Under the zero initial condition, if the following inequality

$$\sum_{k=0}^{\infty} \|\widetilde{e}(k)\|^2 < \gamma^2 \sum_{k=0}^{\infty} \|\omega(k)\|^2$$

holds for all $w(k) \neq 0$, where $\gamma > 0$ is a given disturbance attenuation level and $\widetilde{e}(k) = \begin{bmatrix} e(k) \\ \bar{e}(k) \end{bmatrix}$, then the H_∞ control performance with the index γ of the system (19) can be assured.

Lemma 1: [8] Given a positive scalar ϵ and symmetric matrices T_1 and T_2, if $T_1 \leq 0$ and $T_1 + \bar{\epsilon}T_2 < 0$, then it has

$$T_1 + \epsilon T_2 < 0 \ \text{ for } \ \forall \epsilon \in (0, \bar{\epsilon}].$$

Lemma 2: [46] Given a full rank matrix $B \in \mathbb{R}^{n_x \times n_u}$, the singular value decomposition (SVD) for which can be expressed as

$$B = O \begin{bmatrix} S \\ 0 \end{bmatrix} V^T$$

where $O^T O = I$ and $V^T V = I$, then for matrices $X > 0$, $D \in \mathbb{R}^{n_x \times n_x}$ and $E \in \mathbb{R}^{n_u \times n_x}$, there exists a matrix $\bar{X}$ such that $XB = B\bar{X}$ holds if and only if

$$X = O \begin{bmatrix} D & 0 \\ 0 & E \end{bmatrix} O^T.$$

III. Main Results

In this section, we firstly analyze the sufficient conditions for the system (19) to be stochastically stable with guaranteed H_∞ control performance in Theorems 1–2. Then, we devise the desired observer-based synchronization controllers by calculating the gains of the observers and controllers as outlined in Theorem 3.

Theorem 1: Given scalars $\epsilon > 0$, $\bar{\alpha}_i \in (0, 1)$, c_m $(m = 1, 2, \ldots, l)$, gain matrices $\widetilde{L}_q$ and $\widetilde{Z}_q$ $(q = 1, 2, \ldots, z)$, the stochastic stability of the system (19) can be obtained if there exist positive-define matrices Q_q with compatible dimensions so that the following matrix inequalities hold.

$$\mathbf{A} = \begin{bmatrix} \Psi_{1,1} & * \\ \Psi_{2,1} & \Psi_{2,2} \end{bmatrix} \leq 0 \tag{20}$$

where

$$\Psi_{1,1} = \mathcal{M}_1^T Q_h \mathcal{M}_1 + \bar{\mathcal{M}}_2^T Q_h \bar{\mathcal{M}}_2 - Q_q + \bar{\mathcal{Z}}_1$$

$$\Psi_{2,1} = \ddot{\mathcal{N}}_1^T Q_h \mathcal{M}_1 + \check{\mathcal{N}}_2^T Q_h \bar{\mathcal{M}}_2$$

$$\Psi_{2,2} = \ddot{\mathcal{N}}_1^T Q_h \ddot{\mathcal{N}}_1 + \check{\mathcal{N}}_2^T Q_h \check{\mathcal{N}}_2 + \bar{\mathcal{Z}}_2$$

$$\bar{\mathcal{Z}}_1 = diag\{\widetilde{W}^T\widetilde{W}, 0, 0, 0\}, \quad \bar{\mathcal{Z}}_2 = -\widetilde{I}$$

$$\bar{\mathcal{M}}_2 = \begin{bmatrix} \bar{\mathcal{R}}_1 & 0 & 0 & 0 \end{bmatrix}, \quad \widetilde{W} = diag\{W, W, \ldots, W\}$$

$$\ddot{\mathcal{N}}_1 = \begin{bmatrix} 0 & \vec{\alpha}\widetilde{\Phi}_q^T\widetilde{L}_q^T & 0 & \bar{\alpha}\widetilde{\Phi}_q^T \end{bmatrix}^T$$

$$\check{\mathcal{N}}_2 = \begin{bmatrix} 0 & -\sqrt{\bar{\alpha}\vec{\alpha}}\widetilde{\Phi}_q^T\widetilde{L}_q^T & 0 & \sqrt{\bar{\alpha}\vec{\alpha}}\widetilde{\Phi}_q^T \end{bmatrix}^T$$

$$\bar{\mathcal{R}}_1 = \begin{bmatrix} 0 & \sqrt{\bar{\alpha}\vec{\alpha}}\widetilde{C}^T\widetilde{\Phi}_q^T\widetilde{L}_q^T & 0 & -\sqrt{\bar{\alpha}\vec{\alpha}}\widetilde{C}^T\widetilde{\Phi}_q^T \end{bmatrix}^T.$$

Proof: In consideration of the augmented system described by (19), we construct a Lyapunov function $V(k)$ as

$$V(k) = \chi^T(k) Q_q \chi(k) \tag{21}$$

and define $\Delta V(k) \triangleq V(k+1) - V(k)$. Then, in the case that $w(k) = 0$ and considering the upper bound for the generated deception signals as presented in (7), it can be deduced that

$$\begin{aligned} E\{\Delta V(k)\} &= E\{\chi^T(k+1)Q_h\chi(k+1) - \chi^T(k)Q_q\chi(k)\} \\ &\leq E\{\chi^T(k+1)Q_h\chi(k+1) - \chi^T(k)Q_q\chi(k)\} + x^T(k)\widetilde{W}^T \\ &\quad \times \widetilde{W}x(k) - \phi^T(k)\phi(k) \\ &= E\{[(\mathcal{M}_1 + \mathcal{M}_2)\chi(k) + (\ddot{\mathcal{N}}_1 + \ddot{\mathcal{N}}_2)\phi(k)]^T Q_h[(\mathcal{M}_1 + \mathcal{M}_2) \\ &\quad \times \chi(k) + (\ddot{\mathcal{N}}_1 + \ddot{\mathcal{N}}_2)\phi(k)] - \chi^T(k)Q_q\chi^T(k) + x^T(k)\widetilde{W}^T \\ &\quad \times \widetilde{W}x(k) - \phi^T(k)\phi(k)\} \end{aligned} \tag{22}$$

where

$$\ddot{\mathcal{N}}_2 = \begin{bmatrix} 0 & -\tilde{\alpha}(k)\widetilde{\Phi}_q^T\widetilde{L}_q^T & 0 & \tilde{\alpha}(k)\widetilde{\Phi}_q^T \end{bmatrix}^T.$$

Based on (6), it can be easily obtained that $E\{\tilde{\alpha}(k)\} = 0$ and $E\{\tilde{\alpha}(k)\tilde{\alpha}(k)\} = \bar{\alpha}\vec{\alpha}$. Thus, we can get

$$E\{\Delta V(k)\} \leq \zeta^T(k)\mathbf{A}\zeta(k)$$

where

$$\zeta(k) = \begin{bmatrix} \chi^T(k) & \phi^T(k) \end{bmatrix}^T.$$

Letting $\mathcal{S}(k) \triangleq \zeta^T(k)\mathbf{A}\zeta(k)$, then it has $\mathcal{S}(k) < 0$ if the conditions described by (20) are satisfied. With it, we can further derive that

$$\begin{aligned} &E\{\chi^T(k+1)Q_h\chi(k+1) - \chi^T(k)Q_q\chi(k)\} \\ &\qquad \leq -\lambda_{min}(-\mathcal{S}(k))\chi^T(k)\chi(k) \end{aligned} \tag{23}$$

Authorized licensed use limited to: Southeast University. Downloaded on July 23,2025 at 23:21:32 UTC from IEEE Xplore. Restrictions apply.

By summing both sides of (23) from $k=0$ to ∞, we have

$$\begin{aligned} E\left\{\sum_{k=0}^{\infty}||\chi(k)||^2\right\} &\le (\lambda_{min}(-\mathcal{S}(k))^{-1}\{\chi^T(0)Q_q\chi(0) \\ &\quad - E\{\chi^T(k+1)Q_h\chi(k+1)\} \\ &\le (\lambda_{min}(-\mathcal{S}(k))^{-1}\chi^T(0)Q_q\chi(0) \\ &= \chi^T(0)\mathcal{O}(k)\chi(0). \end{aligned} \tag{24}$$

It is apparently that $\mathcal{O}(k)=(\lambda_{min}(-\mathcal{S}(k))^{-1}Q_q>0$, so the theorem can be proved according to Definition 1. ■

Considering the existence of the external disturbance in the envisioned SPMCN, we then discuss the H_∞ control performance of the system (19) in Theorem 2 based on the results derived in Theorem 1.

Theorem 2: Given scalars $\gamma>0$, $\epsilon>0$, $\bar{\alpha}_i\in(0,1)$, c_m $(m=1,2,\ldots,l)$, gain matrices $\widetilde{L}_q$ and $\widetilde{Z}_q$ $(q=1,2,\ldots,z)$, the stochastic stability with the guaranteed H_∞ control performance of the system (19) can be achieved if there exist positive-define matrices Q_q with suitable dimensions so that the following matrix inequalities hold.

$$\mathbf{B}=\begin{bmatrix}\Pi_{1,1} & * \\ \Pi_{2,1} & \Pi_{2,2}\end{bmatrix}\le 0 \tag{25}$$

where

$$\begin{aligned} \Pi_{1,1} &= \mathcal{M}_1^TQ_h\mathcal{M}_1+\bar{\mathcal{M}}_2^TQ_h\bar{\mathcal{M}}_2-Q_q+\mathcal{Z}_1 \\ \Pi_{2,1} &= \mathcal{N}_1^TQ_h\mathcal{M}_1+\bar{\mathcal{N}}_2^TQ_h\bar{\mathcal{M}}_2 \\ \Pi_{2,2} &= \mathcal{N}_1^TQ_h\mathcal{N}_1+\bar{\mathcal{N}}_2^TQ_h\bar{\mathcal{N}}_2+\mathcal{Z}_2 \\ \bar{\mathcal{N}}_2 &= \begin{bmatrix}0 & 0 \\ \sqrt{\bar{\alpha}\vec{\alpha}}\widetilde{L}_q\widetilde{\Phi}_q\widetilde{D} & -\sqrt{\bar{\alpha}\vec{\alpha}}\widetilde{L}_q\widetilde{\Phi}_q \\ 0 & 0 \\ \sqrt{\bar{\alpha}\vec{\alpha}}\widetilde{\Phi}_q\widetilde{D} & \sqrt{\bar{\alpha}\vec{\alpha}}\widetilde{\Phi}_q\end{bmatrix} \\ \mathcal{Z}_1 &= diag\{\widetilde{W}^T\widetilde{W},\widetilde{I},\widetilde{I},0\} \\ \mathcal{Z}_2 &= diag\{-\gamma^2,-\widetilde{I}\}. \end{aligned}$$

Proof: By selecting the same Lyapunov function and following similar derivation process as in Theorem 1, for all nonzero $w(k)$, if $\mathbf{B}\le 0$, one has

$$\begin{aligned} &E\{\Delta V(k)\}+E\{\widetilde{e}^T(k)\widetilde{e}(k)\}-\gamma^2w^T(k)w(k) \\ &=\zeta_1^T(k)\mathbf{B}\zeta_1(k)\le 0 \end{aligned} \tag{26}$$

where

$$\zeta_1(k)=\begin{bmatrix}\chi^T(k) & \mathcal{U}^T(k)\end{bmatrix}^T.$$

Moreover, by summarizing both sides of (26) for the time instant k from 0 to ∞, it can be gotten that

$$E\{\sum_{k=0}^{\infty}||\widetilde{e}(k)||^2\}\le\gamma^2\sum_{k=0}^{\infty}||w(k)||^2.$$

Then according to Definition 2, the H_∞ control performance of the system (19) with the predefined attenuation level γ is assured. ■

Remark 4: The conditions for the stability and H_∞ control performance of the envisioned SPMCN are provided in Theorem 2, however, the results are derived based on the given observers and controllers' gains. Therefore, in the following Theorem 3, considering the existence of some nonlinear terms in (25), we will adopt linear matrix inequality (LMI) technology to address the nonlinear terms, and thereby determine the gains of the observers and controllers. Meanwhile, we would like to note that the conditions presented in Theorem 2 are ϵ-dependent, but it is generally hard to ascertain the specific value of the SPP [47]. Thus, we will further introduce $\bar{\epsilon}$ to obtain ϵ-independent conditions based on Lemma 1 in Theorem 3. Given that it is reasonably feasible to acquire the upper bound of the SPP, the practicability of the designed synchronization control method can be significantly enhanced.

Theorem 3: Given scalars $\gamma>0$, $\bar{\epsilon}>0$, $\bar{\alpha}_i\in(0,1)$ and c_m $(m=1,2,\ldots,l)$, the stochastic stability with guaranteed H_∞ control performance of the system (19) can be achieved if there exist positive-definite matrices $Q_q=diag\{Q_{q,1},Q_{q,2},Q_{q,3},Q_{q,4}\}$ and X, matrices $\widetilde{S}_q$ and $\widetilde{U}_q$ $(q=1,2,\ldots,z)$ with compatible dimensions, such that the following LMIs

$$\begin{bmatrix}-Q_q+\mathcal{Z}_1 & * & * & * \\ 0 & \mathcal{Z}_2 & * & * \\ \tilde{\mathcal{M}}_1 & \tilde{\mathcal{N}}_1 & Q_h-\mathcal{H}_e\{X\} & * \\ \tilde{\mathcal{M}}_2 & \tilde{\mathcal{N}}_2 & 0 & Q_h-\mathcal{H}_e\{X\}\end{bmatrix}\le 0 \tag{27}$$

can be satisfied with well-designed observer-based controllers which will be given shortly, where

$$\begin{aligned} \tilde{\mathcal{M}}_1 &= \begin{bmatrix}\tilde{\Upsilon}_1 & -\widetilde{B}\widetilde{U}_q & \widetilde{B}\widetilde{U}_q & 0 \\ \tilde{\Upsilon}_2 & \tilde{\Upsilon}_3 & 0 & \tilde{\Upsilon}_4 \\ 0 & -\widetilde{B}\widetilde{U}_q & \tilde{\Upsilon}_1+\widetilde{B}\widetilde{U}_q & 0 \\ \tilde{\Upsilon}_5 & 0 & 0 & X\widetilde{I}-X\widetilde{\Phi}_q\end{bmatrix} \\ \tilde{\mathcal{M}}_2 &= \begin{bmatrix}\tilde{\mathcal{R}}_1 & 0 & 0 & 0\end{bmatrix} \\ \tilde{\mathcal{N}}_1 &= \begin{bmatrix}X\widetilde{H} & 0 \\ X\widetilde{H}-\vec{\alpha}\widetilde{S}_q\widetilde{\Phi}_q\widetilde{D} & -\vec{\alpha}X\widetilde{S}_q\widetilde{\Phi}_q \\ X\widetilde{H} & 0 \\ \vec{\alpha}X\widetilde{\Phi}_q\widetilde{D} & \bar{\alpha}X\widetilde{\Phi}_q\end{bmatrix} \\ \tilde{\mathcal{N}}_2 &= \begin{bmatrix}0 & 0 \\ \sqrt{\bar{\alpha}\vec{\alpha}}\widetilde{S}_q\widetilde{\Phi}_q\widetilde{D} & -\sqrt{\bar{\alpha}\vec{\alpha}}\widetilde{S}_q\widetilde{\Phi}_q \\ 0 & 0 \\ \sqrt{\bar{\alpha}\vec{\alpha}}X\widetilde{\Phi}_q\widetilde{D} & \sqrt{\bar{\alpha}\vec{\alpha}}X\widetilde{\Phi}_q\end{bmatrix} \\ \tilde{\Upsilon}_1 &= X(\widetilde{A}+c_1\widetilde{G}_1+c_2\widetilde{G}_2+\ldots+c_l\widetilde{G}_l)\widetilde{E}_{\bar{\epsilon}} \\ \tilde{\Upsilon}_2 &= \widetilde{S}_q\widetilde{C}-\vec{\alpha}\widetilde{S}_q\widetilde{\Phi}_q\widetilde{C},\quad \tilde{\Upsilon}_3=\tilde{\Upsilon}_1-\widetilde{S}_q\widetilde{C} \\ \tilde{\Upsilon}_4 &= -\widetilde{S}_q(\widetilde{I}-\widetilde{\Phi}_q)-\widetilde{S}_q(\widetilde{I}-\widetilde{\Phi}_q),\quad \tilde{\Upsilon}_5=\vec{\alpha}X\widetilde{\Phi}_q\widetilde{C} \end{aligned}$$

Authorized licensed use limited to: Southeast University. Downloaded on July 23,2025 at 23:21:32 UTC from IEEE Xplore. Restrictions apply.

$$\hat{\mathcal{R}}_1 = \begin{bmatrix} 0 & \sqrt{\bar{\alpha}\vec{\alpha}}\widetilde{C}^T\widetilde{\Phi}_q^T\widetilde{S}_q^T & 0 & -\sqrt{\bar{\alpha}\vec{\alpha}}\widetilde{C}^T\widetilde{\Phi}_q^T X^T \end{bmatrix}^T$$

$$\mathcal{H}_e\{X\} = X + X^T.$$

Proof: Firstly, we can rewrite (25) as

$$\mathcal{Q}_\epsilon + \mathcal{H} \le 0 \tag{28}$$

where

$$\mathcal{Q}_\epsilon = \begin{bmatrix} \bar{\Pi}_{1,1} & * \\ \Pi_{2,1} & \bar{\Pi}_{2,2} \end{bmatrix}, \quad \mathcal{H} = \begin{bmatrix} -Q_q & 0 \\ 0 & \mathcal{Z}_2 \end{bmatrix}$$

$$\bar{\Pi}_{1,1} = \mathcal{M}_1^T Q_h \mathcal{M}_1 + \bar{\mathcal{M}}_2^T Q_h \bar{\mathcal{M}}_2 + \mathcal{Z}_1$$

$$\bar{\Pi}_{2,2} = \mathcal{N}_1^T Q_h \mathcal{N}_1 + \bar{\mathcal{N}}_2^T Q_h \bar{\mathcal{N}}_2.$$

It can be easily observed that $\mathcal{H} < 0$, and thus the following ϵ-independent condition (29) can be derived from (28) based on Lemma 1.

$$\mathcal{Q}_{\bar{\epsilon}} + \mathcal{H} \le 0. \tag{29}$$

According to Schur complete, it is apparent that (29) can be satisfied if and only if

$$\begin{bmatrix} -Q_q + \mathcal{Z}_1 & * & * & * \\ 0 & \mathcal{Z}_2 & * & * \\ \mathcal{M}_1 & \mathcal{N}_1 & -Q_h^{-1} & * \\ \bar{\mathcal{M}}_2 & \bar{\mathcal{N}}_2 & 0 & -Q_h^{-1} \end{bmatrix} \le 0 \tag{30}$$

can be assured. Then, by pre-multiplying and post-multiplying the left side of (30) with $diag\{I, I, X, X\}$ and $diag\{I, I, X^T, X^T\}$, respectively, it can be derived that

$$\begin{bmatrix} -Q_q + \mathcal{Z}_1 & * & * & * \\ 0 & \mathcal{Z}_2 & * & * \\ \hat{\mathcal{M}}_1 & \hat{\mathcal{N}}_1 & -XQ_h^{-1}X^T & * \\ \hat{\mathcal{M}}_2 & \hat{\mathcal{N}}_2 & 0 & -XQ_h^{-1}X^T \end{bmatrix} \le 0 \tag{31}$$

where

$$\hat{\mathcal{M}}_1 = \begin{bmatrix} \hat{\Upsilon}_1 & -X\widetilde{B}\widetilde{K}_q & X\widetilde{B}\widetilde{K}_q & 0 \\ \hat{\Upsilon}_2 & \hat{\Upsilon}_3 & 0 & \hat{\Upsilon}_4 \\ 0 & -X\widetilde{B}\widetilde{K}_q & \hat{\Upsilon}_1 + X\widetilde{B}\widetilde{K}_q & 0 \\ \hat{\Upsilon}_5 & 0 & 0 & X\widetilde{I} - X\widetilde{\Phi}_q \end{bmatrix}$$

$$\hat{\mathcal{M}}_2 = \begin{bmatrix} \hat{\mathcal{R}}_1 & 0 & 0 & 0 \end{bmatrix}$$

$$\hat{\mathcal{N}}_1 = \begin{bmatrix} X\widetilde{H} & 0 \\ X\widetilde{H} - \vec{\alpha}X\widetilde{L}_q\widetilde{\Phi}_q\widetilde{D} & -\vec{\alpha}X\widetilde{L}_q\widetilde{\Phi}_q \\ X\widetilde{H} & 0 \\ \vec{\alpha}X\widetilde{\Phi}_q\widetilde{D} & \bar{\alpha}X\widetilde{\Phi}_q \end{bmatrix}$$

$$\hat{\mathcal{N}}_2 = \begin{bmatrix} 0 & 0 \\ \sqrt{\bar{\alpha}\vec{\alpha}}X\widetilde{L}_q\widetilde{\Phi}_q\widetilde{D} & -\sqrt{\bar{\alpha}\vec{\alpha}}X\widetilde{L}_q\widetilde{\Phi}_q \\ 0 & 0 \\ \sqrt{\bar{\alpha}\vec{\alpha}}X\widetilde{\Phi}_q\widetilde{D} & \sqrt{\bar{\alpha}\vec{\alpha}}X\widetilde{\Phi}_q \end{bmatrix}$$

$$\hat{\Upsilon}_1 = X(\widetilde{A} + c_1\widetilde{G}_1 + c_2\widetilde{G}_2 + \ldots + c_l\widetilde{G}_l)\widetilde{E}_{\bar{\epsilon}}$$

$$\hat{\Upsilon}_2 = X\widetilde{L}_q\widetilde{C} - \vec{\alpha}X\widetilde{L}_q\widetilde{\Phi}_q\widetilde{C}$$

$$\hat{\Upsilon}_3 = \hat{\Upsilon}_1 - X\widetilde{L}_q\widetilde{C}$$

$$\hat{\Upsilon}_4 = -X\widetilde{L}_q(\widetilde{I} - \widetilde{\Phi}_q) - X\widetilde{L}_q(\widetilde{I} - \widetilde{\Phi}_q)$$

$$\hat{\Upsilon}_5 = \vec{\alpha}X\widetilde{\Phi}_q\widetilde{C}$$

$$\hat{\mathcal{R}}_1 = \begin{bmatrix} 0 & \sqrt{\bar{\alpha}\vec{\alpha}}\widetilde{C}^T\widetilde{\Phi}_q^T\widetilde{L}_q^T X^T & 0 & -\sqrt{\bar{\alpha}\vec{\alpha}}\widetilde{C}^T\widetilde{\Phi}_q^T X^T \end{bmatrix}^T.$$

Given that $Q_h = diag\{Q_{h,1}, \ldots, Q_{h,4}\} > 0$, then it has $Q_{h,g}^{-1} > 0\,(g = 1, \ldots, 4)$. Thus, it can be concluded that $(Q_{h,g} - X)Q_{h,g}^{-1}(Q_{h,g} - X)^T = Q_{h,g} - X - X^T + XQ_{h,g}^{-1}X^T \ge 0$, which indicates that $-XQ_{h,g}^{-1}X^T \le Q_{h,g} - \mathcal{H}_e\{X\}$. Furthermore, for $X = O\begin{bmatrix} D & 0 \\ 0 & E \end{bmatrix}O^T$ and $\widetilde{B} = O\begin{bmatrix} S \\ 0 \end{bmatrix}V^T$, in which $O^TO = I$ and $V^TV = I$, it can be inferred that $X\widetilde{B} = \widetilde{B}\bar{X}$ with $\bar{X} = VN^{-1}DNV^T$ based on Lemma 2. By defining $\widetilde{S}_q = X\widetilde{L}_q$, $\widetilde{U}_q = \bar{X}\widetilde{K}_q$, and substituting $-XQ_{h,g}^{-1}X^T$ and $X\widetilde{B}$ in (31) with $Q_{h,g} - \mathcal{H}_e\{X\}$ and $\widetilde{B}\bar{X}$, respectively, (27) can be ultimately obtained. In addition, we can get that $\widetilde{L}_q = X^{-1}\widetilde{S}_q$ and $\widetilde{K}_q = \bar{X}^{-1}\widetilde{U}_q$, which are the designed gains of the observers and controllers. So far, the proof is completed. ■

Remark 5: This paper investigates the problem of secure synchronization control for SPMCNs under the SC protocol. While inspired by some related researches, there are significant differences between it and the existed works. To be specific, although the synchronization control issue for MCNs has been explored in the literature [6], [7], [36], [48], these studies either do not account for the influence of network invulnerability [6], [7], or overlook addressing the data collision introduced by the limited communication bandwidth [36], [48]; moreover, none of them takes the two-time-scale feature of systems into consideration. Focusing on SPSCNs, a mean square synchronization control method has been presented in [10], however, the work is conducted under an idealistic communication environment where data collision and cyberattacks are not considered; to mitigate the effect of data collision, the H_∞ state estimation issues for SPSCNs based on RR protocol and SC protocol have been respectively tackled in [8] and [21], but neither of the two works shares the same objective of designing a secure synchronization control method as our study; furthermore, it is worth noting that the aforementioned researches consider the two-time-scale characteristic of CNs, but neglect the multidimensional relationships between CN nodes, which are comprehensively addressed in our work.

IV. Simulations

In this section, we consider an urban public traffic network that can be modeled by the envisioned SPMCN, and then conduct simulations over it to evaluate the effectiveness of the proposed synchronization control strategy. To be specific, the modeling process of the urban public traffic network and corresponding parameter settings are introduced firstly, then the simulation

Authorized licensed use limited to: Southeast University. Downloaded on July 23,2025 at 23:21:32 UTC from IEEE Xplore. Restrictions apply.

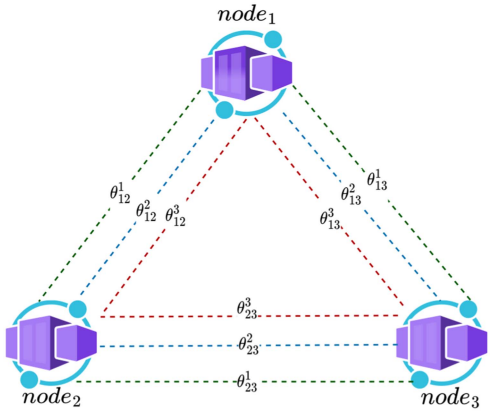

Fig. 2. The modeled urban public traffic system.

results and related illustration are presented to provide a clear understanding.

A. Simulation Modeling and Parameter Settings

An urban public traffic network is generally composed of bus stops and bus lines, thus we regard it as a CN by viewing bus stops as nodes and establishing edges for each pair of nodes which are connected by at least one direct bus line. For the CN, the following three parameters are then defined to reflect the practical relationships between bus stops.

- *Direct service latency:* defined as the maximum waiting time for passengers between two bus stops, which is affected by many factors, e.g., bus frequency and service interruptions. The smaller the latency, the more efficient the bus service.
- *Passenger density:* defined as the average number of passengers between two bus stops, it can be calculated by dividing the total number of passengers between two bus stops during a period of time by the number of bus lines between the two nodes in that period. Passenger density reveals the passenger flow of the area covered by two bus stops.
- *Transfer convenience coefficient:* defined as the number of direct bus lines between two bus stops, which reflects the time cost of transfer. The more the bus lines, the higher the transfer convenience coefficient, and the lower the transfer difficulty for passengers.

By using θ^1_{ij}, θ^2_{ij}, and θ^3_{ij} $(1 \le i, j \le N)$ to represent the above three parameters, and taking the two-time-scale feature into account, the dynamics of the urban public traffic network can be modeled by the SPMCN (1) with $l = 3$. We further set $N = 3$, such a SPMCN is shown in Fig. 2, and assume that three sensors are used for acquiring the state of each $node_i$ which is denoted as $x_i(k) = [x^T_{i1}(k) \quad x^T_{i2}(k) \quad x^T_{i3}(k)]^T$ with $n_s = 1$ and $n_f = 2$ (i.e., $n_y = 3$). The system parameters are defined as below.

$$A = \begin{bmatrix} 0.4506 & 0.1093 & 0.2145 \\ 0.2039 & 0.5167 & 0.5321 \\ 0.0254 & 0.2365 & 0.7415 \end{bmatrix}$$

$$B = \begin{bmatrix} -0.1506 & -0.0193 & 0.2398 \\ 0.3039 & 0.4167 & 0.2145 \\ 0.0124 & 0.05478 & 0.3236 \end{bmatrix}$$

$$C = diag\{0.3, 0.25, 0.4\}, \quad D = diag\{0.2, 0.17, 0.1\}$$

$$H = diag\{0.16, 0.26, 0.1\}, \quad W = diag\{0.1, 0.1, 0.1\}.$$

The coupling strengths are set as $c_1 = 0.02, c_2 = 0.02, c_3 = 0.03$, and the inner-coupling matrices are set to be $\Gamma_1 = diag\{0.4, 0.4, 0.4\}$, $\Gamma_2 = diag\{0.3, 0.3, 0.3\}$, $\Gamma_3 = diag\{0.5, 0.6, 0.6\}$. Based on supposing that $\theta^1_{12} = 3, \theta^1_{13} = 4, \theta^1_{23} = 5, \theta^2_{12} = 5, \theta^2_{13} = 6, \theta^2_{23} = 7, \theta^3_{12} = 4, \theta^3_{13} = 5, \theta^3_{23} = 3.6$, the outer-coupling matrices can be given as

$$\Theta^1 = \begin{bmatrix} -7 & 3 & 4 \\ 3 & -8 & 5 \\ 4 & 5 & -9 \end{bmatrix}, \Theta^2 = \begin{bmatrix} -11 & 5 & 6 \\ 5 & -12 & 7 \\ 6 & 7 & -13 \end{bmatrix}$$

$$\Theta^3 = \begin{bmatrix} -9 & 4 & 5 \\ 4 & -7.6 & 3.6 \\ 5 & 3.6 & -8.6 \end{bmatrix}.$$

The disturbance attenuation level and upper bound of the SPP are determined as $\gamma = 1.5$ and $\bar{\epsilon} = 0.25$. The external disturbance is defined as $w(k) = diag\{-0.4e^{-0.22\,k} sin(0.21\,k), -0.8e^{0.5-0.3\,k} sin(0.21\,k), -0.5\,e^{-0.43\,k} sin(0.41\,k)\}$.

For the adopted SC protocol, the transition probability matrices are defined as

$$P^1 = \begin{bmatrix} 0.25 & ? & ? \\ 0.45 & 0.15 & 0.4 \\ ? & 0.45 & ? \end{bmatrix}, P^2 = \begin{bmatrix} 0.15 & 0.45 & 0.4 \\ ? & 0.35 & ? \\ 0.4 & ? & ? \end{bmatrix}$$

$$P^3 = \begin{bmatrix} ? & 0.4 & ? \\ 0.35 & ? & ? \\ 0.45 & 0.45 & 0.1 \end{bmatrix}.$$

For the considered deception attacks, we set $\bar{\alpha}_1 = 0.4, \bar{\alpha}_2 = 0.3, \bar{\alpha}_3 = 0.5$, and define the attack signals as $\phi_i(k) = 0.1 sin(k-1)x_i(k)$ with energy restriction $W = diag\{0.1, 0.1, 0.1\}$. Moreover, the initial conditions for the isolated node and three system nodes are generated as

$$s(0) = \begin{bmatrix} -0.25 & 0.35 & 0.5 \end{bmatrix}^T$$

$$x_1(0) = \begin{bmatrix} -0.15 & 0.35 & 0.27 \end{bmatrix}^T$$

$$x_2(0) = \begin{bmatrix} -0.35 & 0.25 & -0.1 \end{bmatrix}^T$$

$$x_3(0) = \begin{bmatrix} -0.42 & 0.15 & 0.31 \end{bmatrix}^T$$

$$\hat{x}_1(0) = \begin{bmatrix} 0.15 & -0.35 & -0.2 \end{bmatrix}^T$$

$$\hat{x}_2(0) = \begin{bmatrix} 0.42 & -0.19 & -0.15 \end{bmatrix}^T$$

Authorized licensed use limited to: Southeast University. Downloaded on July 23,2025 at 23:21:32 UTC from IEEE Xplore. Restrictions apply.

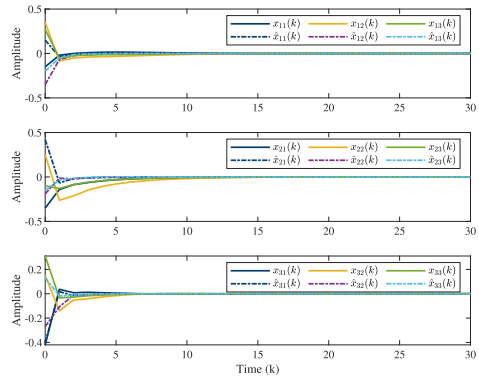

Fig. 3. The system states $x_i(k)$ and observed states $\hat{x}_i(k)$.

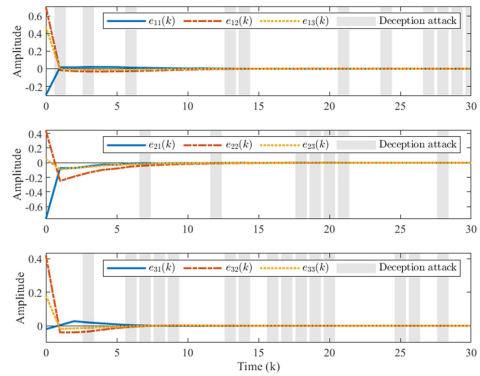

Fig. 4. The observer errors $e_i(k)$ and deception attacks.

$$\hat{x}_3(0) = \begin{bmatrix} -0.4 & -0.27 & 0.13 \end{bmatrix}^T.$$

B. Simulation Results

Based on the above settings, the gain matrices of the observers and controllers, i.e., $L_{i,\psi_i(k)}$ and $K_{i,\psi_i(k)}$ $(i = 1, 2, 3, \psi_i(k) = 1, 2, 3)$, are firstly calculated according to the LMIs given in (27).

Then, the simulation results are shown in Figs. 3–10. Fig. 3 depicts the trends of the system states $x_i(k)$ and their estimations $\hat{x}_i(k)$. As shown, the observed states gradually approach the actual system states within about 10 time instants, which validates the effectiveness of the designed observers. Furthermore, the observer errors $e_i(k)$ under the influence of the deception attacks are displayed in Fig. 4. It can be seen that the observer errors converge to zero after a certain period of time, which further confirms the result given in Fig. 3.

The responses of the synchronization errors $\bar{e}_i(k)$ are presented in Fig. 5. It can be found that the errors also converge to zero with the designed control inputs $u_i(k)$, the trajectories of which are shown in Fig. 6, and thus the efficiency of the proposed synchronization strategy is affirmed. For the considered SC protocol, Fig. 7 shows the index of the authorized sensor for each node at each time instant. It is evident that only one sensor is chosen for data transmission at each time instant, and thereby data conflict can be prevented.

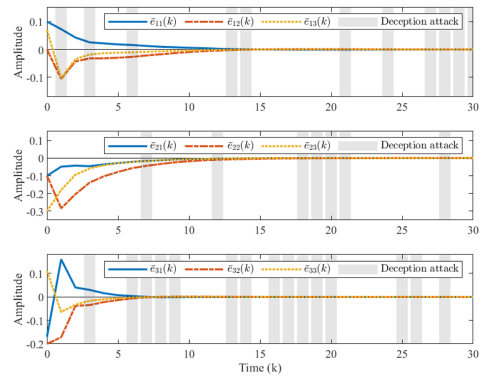

Fig. 5. The synchronization errors $\bar{e}_i(k)$ and deception attacks.

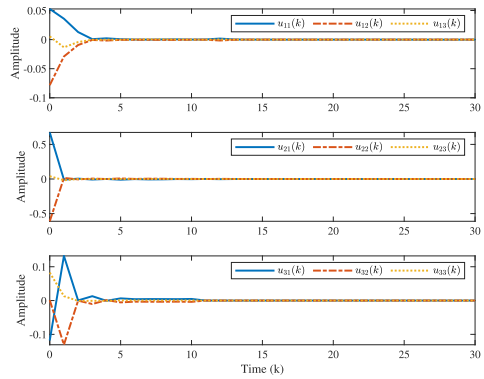

Fig. 6. The trajectories of $u_i(k)$.

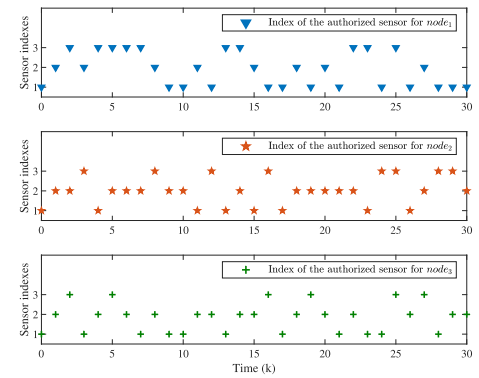

Fig. 7. The indexes of the authorized sensors.

To investigate the influence of the different weights, i.e., θ_{ij}^l $(l = 1, 2, 3;\ 1 \le i, j \le 3)$, on the synchronization control strategy, we then vary the values of one weight while fixing the values of the other two weights at a time, and then show the values of the $||u(k)||$ under the different settings of θ_{ij}^l in Fig. 8. To be specific, the $||u(k)||$ is calculated under four cases, and the values of θ_{ij}^l in each case are given in Table I. As shown, the $||u(k)||$ obtained in cases 2-4 are larger than that obtained in case 1, which means that more control costs need to be paid with the increase of direct service latency (passenger density or transfer convenience coefficient) to synchronize the considered SPMCN.

Authorized licensed use limited to: Southeast University. Downloaded on July 23,2025 at 23:21:32 UTC from IEEE Xplore. Restrictions apply.

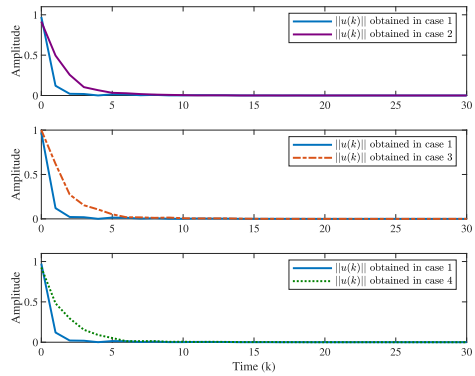

Fig. 8. The comparison of $||u(k)||$.

TABLE I
DIFFERENT SETTINGS OF θ_{ij}^l

Settings	$\{\theta_{12}^1, \theta_{13}^1, \theta_{23}^1\}$	$\{\theta_{12}^2, \theta_{13}^2, \theta_{23}^2\}$	$\{\theta_{12}^3, \theta_{13}^3, \theta_{23}^3\}$
case 1	{3,4,5}	{5,6,7}	{4,5,3.6}
case 2	{19,23,26}	{5,6,7}	{4,5,3.6}
case 3	{3,4,5}	{26,22,21}	{4,5,3.6}
case 4	{3,4,5}	{5,6,7}	{13,16,11}

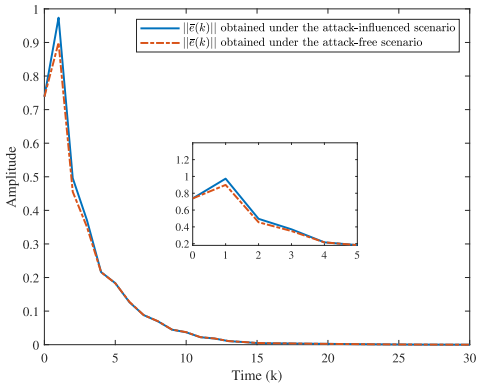

Fig. 9. $||\bar{e}(k)||$ obtained with and without the deception attacks.

It is noted that the above results are obtained under the deception attacks, and there also exist some works that investigate H_∞ synchronization control issue without considering the deception attacks [16], [18]. In view of this, we then conduct a comparative experiment to show the synchronization errors under two scenarios, i.e., the attack-influenced scenario of our study and the attack-free scenario of the listed works. The specific result is presented in Fig. 9, and it can be seen that the $||\bar{e}(k)||$ obtained with the deception attacks is indeed larger than that observed under the attack-free scenario, but the gap between them is quite small. Given the inevitability of cyberattacks due to the inherent openness of communication network, our approach offers a more practical solution for the synchronization control of SPMCNs.

Furthermore, as we stated in Remark 4, the presented synchronization method is devised based on the upper bound of the SPP since that it is hardly realistic to obtain the exact value of the SPP. To specifically verify the feasibility of such a design, we then compare the $||\bar{e}(k)||$ obtained with $\bar{\epsilon}$ as our work and that derived with ϵ as the existed research [9] in Fig. 10. As shown, although the $||\bar{e}(k)||$ acquired with $\bar{\epsilon}$ is slightly greater than that gained with ϵ, it still gradually converges to zero. Notably, the

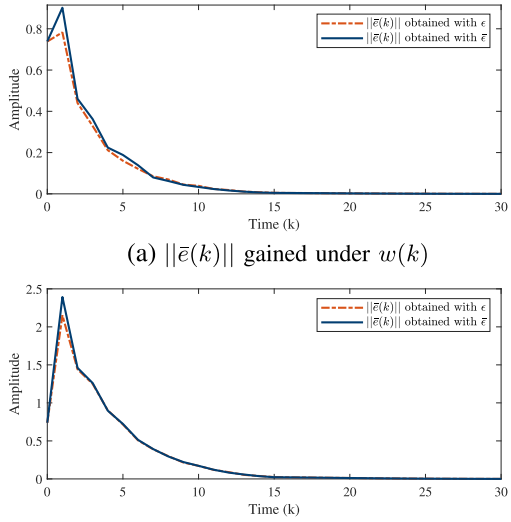

(a) $||\bar{e}(k)||$ gained under $w(k)$

(b) $||\bar{e}(k)||$ gained under $\tilde{w}(k)$

Fig. 10. The comparison of $||\bar{e}(k)||$.

interval between the two becomes small with the increase in the intensity of external disturbance as revealed by Fig. 10(b), where $w(k)$ is amplified into $\tilde{w}(k) = 5w(k)$. This is possible, as the synchronization method designed based on $\bar{\epsilon}$ has sufficient tolerance for the external disturbance. These observations thoroughly validate the practicability of the proposed mechanism.

V. CONCLUSION

In this paper, an observer-based H_∞ synchronization control scheme is proposed for a SPMCN limited by communication resources and deception attacks. Specifically, by implementing a Markov chain-driven SC protocol, the measurement signals generated by multiple sensors in each node are well scheduled and then enabling conflict-free data transmission to mitigate the influence of communication constraints. Moreover, the characteristics of the deception attacks asynchronously launched on each node are effectively depicted by Bernoulli variables and energy bounded functions. Based on these, the distributed observers and controllers are devised, and then the mathematical formulation of the studied synchronization problem is provided via constructing an augmented synchronization error system. Then, the ϵ-independent sufficient conditions for achieving the stochastic stability with guaranteed H_∞ control performance of the system are derived, according to which the gains of the designed observer-based synchronization controllers can be calculated. Simulation results obtained based on a SPMCN-modeled urban public traffic network with the three defined weights are finally presented. As revealed, the proposed synchronization method achieves the desired control performance even under the restricted network environment.

REFERENCES

[1] T. Shanmukhappa, I. Wanghei Ho, C. Tse, and K. Leung, "Recent development in public transport network analysis from the complex network perspective," *IEEE Circuits Syst. Mag.*, vol. 19, no. 4, pp. 39–65, Fourth Quarter 2019.

Authorized licensed use limited to: Southeast University. Downloaded on July 23,2025 at 23:21:32 UTC from IEEE Xplore. Restrictions apply.

[2] J. Chen, Y. Huang, R. Zhang, and Q. Zhu, "Optimal curing strategy for competing epidemics spreading over complex networks," *IEEE Trans. Signal Inf. Process. Netw.*, vol. 7, pp. 294–308, 2021.

[3] Y. Cao, J. Zhuang, M. Jia, X. Zhao, X. Yan, and Z. Liu, "Picture-in-picture strategy-based complex graph neural network for remaining useful life prediction of rotating machinery," *IEEE Trans. Instrum. Meas.*, vol. 72, 2023, Art. no. 2511311.

[4] Y. Liu, Z. Wang, L. Zou, D. Zhou, and W. Chen, "Joint state and fault estimation of complex networks under measurement saturations and stochastic nonlinearities," *IEEE Trans. Signal Inf. Process. Netw.*, vol. 8, pp. 173–186, 2022.

[5] X. Sun et al., "A novel complex network-based graph convolutional network in major depressive disorder detection," *IEEE Trans. Instrum. Meas.*, vol. 71, 2022, Art. no. 2519408.

[6] J. Wang, P. Wei, H. Wu, T. Huang, and M. Xu, "Pinning synchronization of complex dynamical networks with multiweights," *IEEE Trans. Syst., Man, Cybern. Syst.*, vol. 49, no. 7, pp. 1357–1370, Jul. 2019.

[7] X. Liu, "Synchronization and control for multiweighted and directed complex networks," *IEEE Trans. Neural Netw. Learn. Syst.*, vol. 34, no. 6, pp. 3226–3233, Jun. 2023.

[8] X. Wan, Z. Wang, M. Wu, and X. Liu, "H_∞ state estimation for discrete-time nonlinear singularly perturbed complex networks under the round-robin protocol," *IEEE Trans. Neural Netw. Learn. Syst.*, vol. 30, no. 2, pp. 415–426, Feb. 2019.

[9] H. Shen, X. Hu, J. Wang, J. Cao, and W. Qian, "Non-fragile H_∞ synchronization for Markov jump singularly perturbed coupled neural networks subject to double-layer switching regulation," *IEEE Trans. Neural Netw. Learn. Syst.*, vol. 34, no. 5, pp. 2682–2692, May 2023.

[10] K. Liang, W. He, J. Xu, and F. Qian, "Impulsive effects on synchronization of singularly perturbed complex networks with semi-Markov jump topologies," *IEEE Trans. Syst., Man, Cybern. Syst.*, vol. 52, no. 5, pp. 3163–3173, May 2022.

[11] J. Cheng, L. Liang, J. Cao, and Q. Zhu, "Outlier-resistant state estimation for singularly perturbed complex networks with nonhomogeneous sojourn probabilities," *IEEE Trans. Cybern.*, vol. 53, no. 12, pp. 7800–7809, Dec. 2023.

[12] S. Lin and X. Liu, "Generalized decay synchronization of directly coupled stochastic dynamic networks with multiple time delays," *IEEE Trans. Syst., Man, Cybern. Syst.*, vol. 53, no. 4, pp. 2423–2433, Apr. 2023.

[13] S. Lin and X. Liu, "Output synchronization and PID control for directed networks with multiple communications," *IEEE Trans. Syst., Man, Cybern. Syst.*, vol. 55, no. 3, pp. 1620–1633, Mar. 2025.

[14] S. Liu, T. Xu, and E. Tian, "Event-based pinning synchronization control for time-delayed complex dynamical networks: The finite-time boundedness," *IEEE Trans. Signal Inf. Process. Netw.*, vol. 7, pp. 730–739, 2021.

[15] L. Zhao, J. Wang, and Y. Zhang, "Lag output synchronization for multiple output coupled complex networks with positive semidefinite or positive definite output matrix," *J. Franklin Inst.*, vol. 357, no. 1, pp. 414–436, 2020.

[16] Z. Qin, J. Wang, Y. Huang, and S. Ren, "Analysis and adaptive control for robust synchronization and H_∞ synchronization of complex dynamical networks with multiple time-delays," *Neurocomputing*, vol. 289, pp. 241–251, 2018.

[17] J. Wang, Z. Qin, H. Wu, T. Huang, and P. Wei, "Analysis and pinning control for output synchronization and H_∞ output synchronization of multiweighted complex networks," *IEEE Trans. Cybern.*, vol. 49, no. 4, pp. 1314–1326, Apr. 2019.

[18] J. Wang, Z. Qin, H. Wu, and T. Huang, "Finite-time synchronization and H_∞ synchronization of multiweighted complex networks with adaptive state couplings," *IEEE Trans. Cybern.*, vol. 50, no. 2, pp. 600–612, Feb. 2020.

[19] L. Zhao and J. Wang, "Lag H_∞ synchronization and lag synchronization for multiple derivative coupled complex networks," *Neurocomputing*, vol. 384, pp. 46–56, 2020.

[20] C. Jia, J. Hu, B. Li, H. Liu, and Z. Wu, "Recursive state estimation for nonlinear coupling complex networks with time-varying topology and round-robin protocol," *J. Franklin Inst.*, vol. 359, no. 11, pp. 5575–5595, 2022.

[21] X. Wan, Y. Li, Y. Li, and M. Wu, "Finite-time H_∞ state estimation for two-time-scale complex networks under stochastic communication protocol," *IEEE Trans. Neural Netw. Learn. Syst.*, vol. 33, no. 1, pp. 25–36, Jan. 2022.

[22] H. Geng, Z. Wang, F. Alsaadi, K. Alharbi, and Y. Cheng, "Federated tobit kalman filtering fusion with dead-zone-like censoring and dynamical bias under the round-robin protocol," *IEEE Trans. Signal Inf. Process. Netw.*, vol. 7, pp. 1–16, 2021.

[23] L. Zha, T. Huang, J. Liu, E. Tian, X. Xie, and C. Peng, "Secure state estimation for interval type-2 fuzzy systems with FDI attacks and event-triggered WTOD protocol," *IEEE Trans. Syst., Man, Cybern. Syst.*, early access, May 22, 2025, doi: 10.1109/TSMC.2025.3569725.

[24] W. Chen, J. Hu, X. Yu, D. Chen, and Z. Wu, "Robust fault detection for uncertain delayed systems with measurement outliers under stochastic communication protocol," *IEEE Trans. Signal Inf. Process. Netw.*, vol. 8, pp. 684–701, 2022.

[25] X. Ren, G. Yang, and X. Zhang, "Statistical-based optimal ϵ-stealthy attack under stochastic communication protocol: An application to networked permanent magnet synchronous machine systems," *IEEE Trans. Ind. Electron.*, vol. 70, no. 1, pp. 1036–1046, Jan. 2023.

[26] F. Alsaadi, Z. Wang, D. Wang, F. Alsaadi, and F. Alsaade, "Recursive fusion estimation for stochastic discrete time-varying complex networks under stochastic communication protocol: The state-saturated case," *Inf. Fusion*, vol. 60, pp. 11–19, 2020.

[27] D. Du et al., "Co-design secure control based on image attack detection and data compensation for networked visual control systems," *IEEE Trans. Instrum. Meas.*, vol. 71, 2022, Art. no. 3524314.

[28] M. Elsisi, M. Altius, S. Su, and C. Su, "Robust Kalman filter for position estimation of automated guided vehicles under cyberattacks," *IEEE Trans. Instrum. Meas.*, vol. 72, 2023, Art. no. 1002612.

[29] H. Geng, Z. Wang, F. Alsaadi, K. Alharbi, and Y. Cheng, "Protocol-based fusion estimator design for state-saturated systems with dead-zone-like censoring under deception attacks," *IEEE Trans. Signal Inf. Process. Netw.*, vol. 8, pp. 37–48, 2022.

[30] J. Liu, Y. Dong, L. Zha, X. Xie, and E. Tian, "Reinforcement learning-based tracking control for networked control systems with DoS attacks," *IEEE Trans. Inf. Forensics Secur.*, vol. 19, pp. 4188–4197, 2024.

[31] J. Hu, S. Yang, R. CaballeroÁguila, H. Dong, and B. Wu, "Mixed static-dynamic protocol-based tobit recursive filtering for stochastic nonlinear systems against random false data injection attacks," *IEEE Trans. Signal Inf. Process. Netw.*, vol. 10, pp. 445–459, 2024.

[32] J. Feng, J. Xie, J. Wang, and Y. Zhao, "Secure synchronization of stochastic complex networks subject to deception attack with nonidentical nodes and internal disturbance," *Inf. Sci.*, vol. 547, pp. 514–525, 2021.

[33] L. Zhou, M. Huang, F. Tan, and Y. Zhang, "Mean-square bounded synchronization of complex networks under deception attacks via pinning impulsive control," *Nonlinear Dyn.*, vol. 111, no. 12, pp. 11243–11259, 2023.

[34] Y. Li, F. Song, J. Liu, X. Xie, E. Tian, and S. Fei, "Round robin-based synchronization control for discrete-time complex networks with probabilistic coupling delay and deception attacks," *IEEE Trans. Syst., Man, Cybern. Syst.*, vol. 54, no. 7, pp. 4425–4436, Jul. 2024.

[35] R. Sakthivel, O. Kwon, M. Park, S. Choi, and R. Sakthivel, "Event-triggered fault estimation and nonfragile synchronization control for multiweighted complex dynamical networks with deception attacks," *Int. J. Robust Nonlinear Control*, vol. 32, no. 15, pp. 8576–8599, 2022.

[36] R. Sakthivel, O. Kwon, M. Park, and R. Sakthivel, "Event-triggered synchronization control for fractional-order IT2 fuzzy multi-weighted complex dynamical networks with deception attacks," *Commun. Nonlinear Sci. Numer. Simul.*, vol. 136, 2024, Art. no. 108091.

[37] Z. Zhang, Y. Niu, Z. Cao, and J. Song, "Security sliding mode control of interval type-2 fuzzy systems subject to cyber attacks: The stochastic communication protocol case," *IEEE Trans. Fuzzy Syst.*, vol. 29, no. 2, pp. 240–251, Feb. 2021.

[38] J. Liu, J. Ke, J. Liu, X. Xie, and E. Tian, "Secure event-triggered control for IT-2 fuzzy networked systems with stochastic communication protocol and FDI attacks," *IEEE Trans. Fuzzy Syst.*, vol. 32, no. 3, pp. 1167–1180, Mar. 2024.

[39] Y. Yuan, Z. Wang, P. Zhang, and H. Liu, "Near-optimal resilient control strategy design for state-saturated networked systems under stochastic communication protocol," *IEEE Trans. Cybern.*, vol. 49, no. 8, pp. 3155–3167, Aug. 2019.

[40] J. Zhang, C. Peng, M. Fei, and Y. Tian, "Output feedback control of networked systems with a stochastic communication protocol," *J. Franklin Inst.*, vol. 354, no. 9, pp. 3838–3853, 2017.

[41] B. Shen, Z. Wang, D. Wang, and Q. Li, "State-saturated recursive filter design for stochastic time-varying nonlinear complex networks under deception attacks," *IEEE Trans. Neural Netw. Learn. Syst.*, vol. 31, no. 10, pp. 3788–3800, Oct. 2020.

[42] C. Hu, S. Ding, and X. Xie, "Event-based distributed set-membership estimation for complex networks under deception attacks," *IEEE Trans. Automat. Sci. Eng.*, vol. 21, no. 3, pp. 3719–3729, Jul. 2024.

Authorized licensed use limited to: Southeast University. Downloaded on July 23,2025 at 23:21:32 UTC from IEEE Xplore. Restrictions apply.

[43] X. Li, G. Wei, D. Ding, and S. Liu, "Recursive filtering for time-varying discrete sequential systems subject to deception attacks: Weighted try-once-discard protocol," *IEEE Trans. Syst., Man, Cybern. Syst.*, vol. 52, no. 6, pp. 3704–3713, Jun. 2022.

[44] Z. Wu, P. Shi, Z. Shu, H. Su, and R. Lu, "Passivity-based asynchronous control for Markov jump systems," *IEEE Trans. Autom. Control*, vol. 62, no. 4, pp. 2020–2025, Apr. 2017.

[45] Y. Luo, F. Deng, Z. Ling, and Z. Cheng, "Local H_∞ synchronization of uncertain complex networks via non-fragile state feedback control," *Math. Comput. Simul.*, vol. 155, pp. 335–346, 2019.

[46] L. Zha, R. Liao, J. Liu, X. Xie, E. Tian, and J. Cao, "Dynamic event-triggered output feedback control for networked systems subject to multiple cyber attacks," *IEEE Trans. Cybern.*, vol. 52, no. 12, pp. 13800–13808, Dec. 2022.

[47] J. Cheng, W. Huang, H. K. Lam, J. Cao, and Y. Zhang, "Fuzzy-model-based control for singularly perturbed systems with nonhomogeneous Markov switching: A dropout compensation strategy," *IEEE Trans. Fuzzy Syst.*, vol. 30, no. 2, pp. 530–541, Feb. 2022.

[48] R. Sakthivel, O.-M. Kwon, M.-J. Park, and S. Lee, "Disturbance rejection for multi-weighted complex dynamical networks with actuator saturation and deception attacks via hybrid-triggered mechanism," *Neural Netw.*, vol. 162, pp. 225–239, 2023.

Authorized licensed use limited to: Southeast University. Downloaded on July 23,2025 at 23:21:32 UTC from IEEE Xplore. Restrictions apply.